Journal of Simulation and Analysis of Novel Technologies in Mechanical Engineering
15 (1) (2023) 0063~0077

Research article

Lattice Boltzmann method for natural convection of nanofluid flow in a trapezoidal-shaped sinusoidal cavity by considering Brownian motion

Nemat Ebrahimi[1], Hossein Ahmadi Danesh Ashtiani[1]*, Davood Toghraie[2]

[1]*Department of Mechanical Engineering, South Tehran Branch, Islamic Azad University, Tehran, Iran*

[2]*Department of Mechanical Engineering, Khomeinishahr Branch, Islamic Azad University, Khomeinishahr, Iran*

* h_a_danesh@azad.ac.ir

(Manuscript Received --- 12 Dec. 2022; Revised --- 20 Dec.2022; Accepted --- 31 Dec. 2022)

Abstract

Using the lattice Boltzmann technique, the mixed convection of nanofluid inside an inclined trapezoidal cavity in the presence of a multidirectional magnetic field is investigated. The sides of the trapezoidal hollow are adiabatic, with the upper moveable wall being cold and the lower wall being sinusoidally heated. In simulations, the temperature and flow distribution functions are utilized to determine all parameters related to the temperature and flow fields. On the hot wall, the effects of various Rayleigh numbers (Ra = 10^3, 10^4, and 10^5), inclined cavity angles (θ= 0°-90°), volume fractions of nanoparticles (ϕ== 0-3 percent), magnetic field intensity (Ha = 0-100), and applied magnetic field angle (θ= 0°-90°) were studied. According to the research, raising the Rayleigh number enhances heat transfer. Moreover, when all other parameters are held equal, raising the nanoparticle volume fraction enhances the average Nusselt number. As results show, increasing nanoparticle can increase heat transfer by 10 percent but, As the percentage of the nanoparticles rises, this reduction may be brought about by a decrease in the Brownian motion of the particles. Then, as the nanoparticle size goes beyond 2%, the thermal conductivity starts to rise. An increase in diffusive heat transfer may be the source of this rise in thermal conductivity. Increasing the Hartmann number reduces the flow velocity inside the cavity, hence reducing heat transfer dramatically by 50 percent when Ra number is high. Changes in the cavity's slope and the angle of the applied magnetic field have an effect on the flow and heat transfer as well.

Keywords: Lattice Boltzmann method, Natural convection, Trapezoidal cavity, Nanofluid

Nomenclatures

c_i(m/s)	the discrete velocity of Boltzmann grid
$c_p(m/s)$	specific heat at constant pressure
c_s(m/s)	sound speed
d_p(nm)	nanoparticle diameter
$F(J)$	buoyancy force
f_i	the distribution function
f_i^{eq}	the local equilibrium distribution function
$g_y(m/s^2)$	the gravitational acceleration
g_i	temperature distribution function

g_i^{eq}	i the local equilibrium distribution function of temperature
Gr	Grashof Number
$k\ (W/m^2.K)$	conduction heat transfer coefficient
L(m)	the width of the cavity
Nu	Nusselt number
Pr	Prandtl Number
Ra	Rayleigh number
Ha	Hartman number
T(K)	Temperature
t(s)	Time
u(m/s)	velocity component in the x-direction
$v(m/s)$	velocity component in the y-direction
$u_0(m/s)$	The velocity of the top wall
w_i	the weight function of the i_{th} direction

Greek

$\alpha\ (m^2/s)$	thermal diffusivity
β (1/K)	coefficient of thermal expansion
$\mu\ (m^2/s)$	Viscosity
θ	Dimensionless temperature
Θ	Inclination angle
ρ (kg/m^3)	Density
γ	The angle of applied Magnetic force
φ	the volume fraction of nanoparticles
τ_v	the relaxation time of the flow field
τ_D	the relaxation time of the temperature field
ν	Kinematic viscosity
Δx	Spatial step
Δt	Time step

Footnotes

avg	Average
C	Cold
f	Fluid
H	Hot
nf	Nanofluid
s	Nanoparticle
w	Wall

1- Introduction

In industrial and scientific applications, the natural and forced heat transfer mechanisms are the most significant fluxes. Natural convection is relevant in a range of industries, such as the refrigeration industry and air conditioning systems, due to its simplicity, inexpensive cost, and minimal noise. In addition, forced convective heat transfer is relevant to drying processes and heat exchangers, which are often linked with natural heat transfer. In a hollow with a sliding lid, mixed heat transfer is caused by two factors: the production of shear flow owing to moving walls and the buoyancy force due to temperature boundary conditions [1-3]. In order to increase the heat transfer efficiency, nanofluids are utilized in place of conventional fluids due to equipment space constraints.

Choi [4] advocated adding nanoparticles to the base fluid to increase the conductivity of fluids in industrial applications. Heris et al. [5] studied experimentally the nanofluid driven convective heat transfer. They determined that the type and size of nanoparticles, the kind of base fluid, the flow regime, and the boundary conditions had a significant impact on the heat transfer parameters, such as the Nusselt number. Zarringhalam et al. [6] performed studies on nanofluids with varied volume fractions and observed that increasing the nanoparticle volume fraction enhances the Nusselt number and heat transfer rate of conventional fluids. Esfe et al. [7] conducted an experiment to determine the impact of Al2O3 nanoparticles in ethylene glycol on energy equipment. In addition, they investigated the influence of nanoparticle volume fraction, temperature, and nanoparticle size on the conductivity coefficient and viscosity of nanofluids.

Using the lattice Boltzmann technique, Kefayati et al. [8] conducted a computational examination of nanofluid heat transfer within a cavity filled with CiO2-water nanofluid. In a cavity with an aspect ratio of 0.5-2, they evaluated the convective heat transfer at Ra values between 103 and 105. Nemati et al. [9] investigated the impact of nanoparticle volume fraction in a cavity filled with CuO and Al2O3 nanofluids. They observed that the volume percentage of CuO has a greater influence than other nanofluids. Despite the fact that the majority of research in this topic are undertaken in square geometries, certain examinations have been conducted

in different geometries. Hasib et al. [10] investigated the mixed heat transfer of nanofluid within a trapezoidal-shaped cavity and reported the influence of nanoparticle volume fraction and Ri on the heat transfer. Yuan Ma et al. [11] used LBM to solve the governing equations of laminar forced convective heat transfer of nanofluid via a bent channel and demonstrated that the local and average Nusselt number rises as the Ri number increases.

Most studies have shown that increasing the nanoparticle volume percentage improves heat transfer [12-15]. Therefore, the electro-hydro magnetic force may be used to regulate and control heat transfer and flow parameters. According to the frequent use of natural and forced convective heat transfer, many geometries for natural heat transfer were examined. The majority of these research are conducted in constant-temperature 2-D cavities. As nuclear reactor design technology advances, the influence of magnetic field on heat transfer becomes more significant. It is recognized that MHD fluxes alter the flow and heat transfer of fluids. Mahmoudi et al. [16] simulated an MHD flow and heat transfer within a 2-D cavity filled with Al2O3 nanofluid. They determined that heat transfer has a direct relationship with Ra and an inverse relationship with Ha. Kefayati et al. [17] studied the mixed convection of nanofluids driven by a magnetic field within a rectangular chamber heated linearly from one side. They discovered that increasing Ha number decreases heat transfer, whereas increasing Richardson number enhances it. They demonstrated that the application of a magnetic field is the most important component in reducing heat transfer. Yuan Ma et al. [18] explored the influence of heaters and coolers on temperature distribution in a channel filled with Ag-MgO/water nanofluid, as well as the impact of Ra, Re, and Ha numbers on streamlines and isotherms. They demonstrated that increasing the direction that magnetic force applies, increases heat transfer.

Mehryan et al. [19] investigate the effects of Cu-Al2O3/water hybrid nanofluid and Al2O3/water nanofluid on mixed convection induced by a heated oscillating cylinder within a square cavity and tried to quantify the impacts of several factors, including the nanoparticle volume percentage, the Rayleigh number, the amplitude of the oscillation, and the oscillation period of the cylinder. The average Nusselt number rises when the Rayleigh number is low due to the oscillating cylinder's motion toward the top and bottom walls. In addition, when the Rayleigh number is low, the inclusion of Al2O3 and Cu-Al2O3 nanoparticles increases the average Nusselt number. Saliha and Rachid [20] investigated convective heat transfer and entropy formation in an open cubic cavity filled with a hybrid nanofluid using numerical simulation. To continuously heat the arrangement, a volumetric heat source was used.

Mehryan et al. [21] investigated natural convection of Ag-MgO/water nanofluids in a porous medium and evaluated the effects of local thermal non-equilibrium in a porous medium. They discovered that heat transfer is impeded by the presence of Ag–MgO hybrid nanoparticles in water. Mehryan et al. [22] also examined a suspension of Nano–Encapsulated Phase Change Materials (NEPCMs) in an eccentric annulus cage. They observed that NEPCM particles enhance heat transfer.

Rahman [23] used GPU-accelerated MRT-LBM to model the natural convection and entropy generation of non-Newtonian

nanofluids with varying magnetic field angles. They demonstrated that the average Nusselt number increases with rising power-law index values, reaches a maximum at n = 1, and then starts to decrease as the fluid shear-thickens. Finally, the entropy profile of the research is thoroughly examined.

Rahimi et al. [24] modeled natural convection heat transfer and fluid flow using the lattice Boltzmann numerical technique. In their study, they use entropy generation analysis and heat line visualization to explore the convective flow field in depth. The hollow L-shaped cavity is considered and filled with SiO2-TiO2/Water-EG nanofluid. Experimentally determining the thermal conductivity and dynamic viscosity of a nanofluid.

Hussain et al. [25] did study on the numerical estimation of three-dimensional unsteady laminar natural convection and entropy generation in an inclined cubical trapezoidal air-filled cavity. Increasing the Rayleigh number modifies the flow patterns, particularly in three-dimensional results, and improves flow circulation. In addition, when the Rayleigh number is low, the impact of the inclination angle on the formation of total entropy becomes insignificant. In addition, as the Rayleigh number increases, the average Nusselt number increases as well.

Selimefendigil et al. [26] analyzed the mixed convection of a CuO–water nanofluid-filled, lid-driven cavity with upper and lower triangular domains under the influence of angled magnetic fields. The top horizontal wall of the cavity travels at a constant velocity of uw in the +x direction, but the other walls are subject to no-slip boundary conditions. According to the results, when the Hartmann number and magnetic angle of the top triangle are raised, the averaged transfer declines more than in the lower triangle. When the heat transfer rate is high and convection is not reduced by reducing the Hartmann number, they demonstrated that inserting nanoparticles is more effective for enhancing local heat transfer. In addition, a second law analysis is performed on the system for different combinations of flow parameters.

In the current study, the simulation of natural heat transfer of ethylene glycol-Fe nanofluid is implemented inside an inclined cavity heated sinusoidally from the lower wall in the presence of a magnetic field in different directions by employing a model that considers the behavior of nanofluid based on the Brownian motions of molecules. Numerous scientists utilized multiple models to predict the behavior of nanofluids, but the majority of these models did not account for the effects of temperature and paricle diameter. In contrast, the KKL model, which considers Brownian motion for nanoparticles, is utilized in this study. In this simulation, the effect of nanofluid on the enhancement of heat transfer in the presence of a magnetic field is investigated. In addition, the effect of the Ra number, the nanoparticle volume fraction, the Ha number, and the angle of the applied magnetic field are investigated in the trapezoidal cavity in order to design the most suitable systems. Due to the application of this geometry on the fins of specialized heat exchangers in the oil industry, the present study investigates the heat transfer of trapezoidal-shaped sinusoidal heated from below.

2- Problem Statement

The geometry of the current issue is shown in Fig. 1. This trapezoid-shaped cavity is sloped. The bottom horizontal wall is heated sinusoidally to a temperature of T_h.

The top horizontal wall has a cool T_c temperature, but the left and right walls are adiabatic. According to the geometry, the z-direction heat transfer is insignificant and the assumption of two-dimensional flow is valid. At an average temperature of 300 K, the cavity contains ethylene glycol-Fe nanofluids. The flow is laminar, and a magnetic field is supplied to the cavity at an angle of γ with respect to the horizon. The base of the cavity has a length L and a height H, and the adjacent angles are 45 degrees. Table 1 provides the nanofluids thermophysical properties

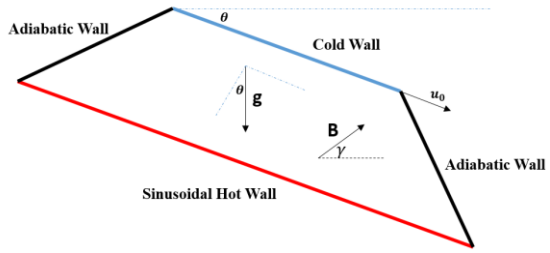

Fig. 1 Problem geometry

Table 1: Thermo-physical properties of the fluid (ethylene glycol) and nanoparticles (Fe) [7]

Properties	EG	Fe
ρ (kg/m^3)	1114	7900
C_p (J/kg K)	2415	444
$K\ (W/m.K)$	0.252	80
$d_p(nm)$	–	47

3- Lattice Boltzmann Method

LBM is one of the most powerful numerical algorithms in fluid simulation and is used to analyze a wide range of issues and challenges. The lattice Boltzmann approach, unlike earlier numerical methods, is based on microscopic models and mesoscopic kinetic equations. The lattice Boltzmann technique has been used to simulate multiphase currents. Due to the complexity of heterogeneous flows, it is difficult to simulate them using typical numerical approaches, such as the macroscopic Navier-Stokes solution. Due of its kinetic nature, lattice Boltzmann can handle such challenges. The Lattice Boltzmann $D_2\ Q_9$ model was employed for flow and temperature in this study. Two distribution functions meeting continuity, momentum, and energy equations on a macroscopic scale are selected for flow field and temperature [27].

$$\frac{\partial u^*}{\partial x^*}+\frac{\partial v^*}{\partial y^*}=0 \tag{1}$$

$$\rho_{nf}\left(u^*\frac{\partial u^*}{\partial x^*}+v^*\frac{\partial u^*}{\partial y^*}\right) = -\frac{\partial p}{\partial x^*} + \mu_{nf}\left(\frac{\partial^2 u^*}{\partial x^{*2}}+\frac{\partial^2 u^*}{\partial y^{*2}}\right)+F_x \tag{2}$$

$$\rho_{nf}\left(u^*\frac{\partial u^*}{\partial x^*}+v^*\frac{\partial u^*}{\partial y^*}\right) = -\frac{\partial p}{\partial x^*} + \mu_{nf}\left(\frac{\partial^2 u^*}{\partial x^{*2}}+\frac{\partial^2 u^*}{\partial y^{*2}}\right)+F_x \tag{3}$$

$$u^*\frac{\partial T^*}{\partial x^*}+v^*\frac{\partial T^*}{\partial y^*}=\alpha_{nf}\left(\frac{\partial^2 T^*}{\partial x^{*2}}+\frac{\partial^2 T^*}{\partial y^{*2}}\right) \tag{4}$$

where $u^*=\frac{u}{u0}$, $y^*=y/L$ and $x^*=x/L$ are non-dimensional velocity and space coordinates. The Lattice Boltzmann equations can be written using Equation BGK for the flow field to which external forces have been applied as Equation (5) [27]:

$$f_i(x+c_i\Delta t,t+\Delta t)=f_i(x,t) + \frac{\Delta t}{\tau_v}[f_i^{eq}(x,t)-f_i(x,t)] + \Delta t c_i F_i \tag{5}$$

And for the temperature field, the following relation is established [27]:

$$g_i(x + c_i\Delta t, t + \Delta t) = g_i(x,t) + \frac{\Delta t}{\tau_D}\left[g_i^{eq}(x,t) - g_i(x,t)\right] \quad (6)$$

where Δt is the time step of the geometry, c_i is the discrete speed of the geometry in the direction of i, F_i is the external force in the direction of the geometry speed, and τ_v and τ_D are the relaxation time for the flow field and temperature, respectively. f and g are two distribution functions, which are used for momentum and energy equations, respectively. In the above expressions, f_i^{eq} and g_i^{eq} are equilibrium distribution functions that are presented as follows [27].

$$f_i^{eq} = w_i\rho_{nf}\left[1 + \frac{c_i.u}{c_s^2} + \frac{1}{2}\frac{(c_i.u)^2}{c_s^4} - \frac{1}{2}\frac{u^2}{c_s^2}\right] \quad (7)$$

$$g_i^{eq} = w_i T\left[1 + \frac{c_i.u}{c_s^2}\right] \quad (8)$$

where ρ_{nf} is the nanofluid density, T is the temperature and u is the macroscopic velocity. According to the definition of geometry D_2Q_9 (Fig. 2), c_i and w_i are defined as follows:

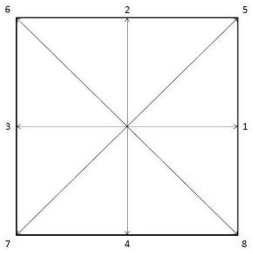

Fig. 2 D_2Q_9 lattice

$$c_i = \begin{Bmatrix} 0 & i = 0 \\ c\left(\cos\left[(i-1)\frac{\pi}{2}\right], \sin\left[(i-1)\frac{\pi}{2}\right]\right) & i = 1-4 \\ c\left(\cos\left[(i-5)\frac{\pi}{2} + \frac{\pi}{4}\right], \sin\left[(i-5)\frac{\pi}{2} + \frac{\pi}{4}\right]\right) & i = 5-8 \end{Bmatrix} \quad (9)$$

$$w_i = \begin{Bmatrix} 4/9 & i = 0 \\ 1/9 & i = 1-4 \\ 1/36 & i = 5-8 \end{Bmatrix} \quad (10)$$

where $c = \frac{\Delta x}{\Delta t}$ and Δx and Δt are spatial and time steps in the Lattice Boltzmann unit, respectively, which are equal to one. The relaxation time of the flow field and temperature equations is obtained from the following equation [27].

$$\tau_v = 3\nu_{nf}(lbm) + 0.5 \quad (11)$$

$$\tau_D = 3\alpha_{nf}(lbm) + 0.5 \quad (12)$$

The effect of buoyant force and the presence of magnetic force is added to Equation (5) as a source expression [27].

$$F = F_x + F_y \quad (13)$$

$$F_x = 3w_i\rho_f A(v sin\gamma cos\gamma - u sin^2\gamma) + 3w_i g sin\theta(\rho\beta)_{nf}\theta \quad (14)$$

$$F_y = 3w_i\rho_f A(u sin\gamma cos\gamma - v cos^2\gamma) + 3w_i g cos\theta(\rho\beta)_{nf}\theta \quad (15)$$

where

$$A = Ha^2\left(\frac{\mu_{nf}}{H^2}\right) \quad (16)$$

$$\theta = \frac{T - T_h}{T_h - T_c} \quad (17)$$

Ha is the Hartmann number, γ is the inclination angle of the magnetic field, H is the characteristic length, and x and y represent the directions of the coordinate axes. Finally, macroscopic quantities are calculated using the solution of distribution functions [27].

$$\rho = \sum_i f_i \quad (18)$$

$$\rho\boldsymbol{u_j} = \sum_{\boldsymbol{i}} f_i\boldsymbol{c_{ij}} \quad (19)$$

$$T = \sum_i g_i \quad (20)$$

The Nu number is one of the most important dimensionless numbers in describing the rate of heat transfer, which is calculated as Equation (21) on a hot wall [27].

$$Nu_{avg} = \frac{1}{H}\int_0^1 -\frac{k_{nf}}{k_f}\left(\frac{\partial\theta}{\partial X}\right)_{X=0} dY \quad (21)$$

As is showed in Fig. (1), The upper wall is moving with a non-null velocity. Normally there is a heat dissipation term in the energy equation source term. The Eckert number is used to describe the impact of self-heating of a fluid due to dissipation effects. At high flow velocities, the temperature profile in a fluidic system is dominated not only by the temperature gradients existing in the system, but also by the effects of dissipation owing to fluid internal friction. The Eckert number determines whether the consequences of self-heating due to dissipation may be ignored (Ec<<1) or not. Eckert number is defined as: $Ec = \frac{u^2}{c_v(T_h - T_c)}$ which In LBM units, c_v and $(T_h - T_c)$ are considered to be equal to 1. By considering the definition of Ra, Re and Ri numbers, it is noted that for simulation of natural convection Ec=0 and in mixed convection for Ri=10, Ec is equal to $Ec = 3.86 \times 10^{-5}$ and when Ri=0.1, $Ec = 0.0038$. As we can see, in both conditions, $Ec \ll 1$. Thus, self-heating due to dissipation can be neglected. The effective density (ρ_{nf}), the coefficient of thermal expansion ($\rho\beta_{nf}$), the thermal capacitance ($\rho c_{p_{nf}}$), the viscosity (ν_{nf}) and the Thermal diffusivity of the nanofluid (α_{nf}) are calculated using equations (28) o (32) [7]:

$$\rho_{nf} = (1-\varphi)\rho_f + \varphi\rho_s \quad (22)$$

$$(\rho c_p)_{nf} = (1-\varphi)\rho c_{p_f} + \varphi\rho c_{p_s} \quad (23)$$

$$(\rho\beta)_{nf} = (1-\varphi)\rho\beta_f + \varphi\rho\beta_s \quad (24)$$

$$\nu_{nf} = \frac{\mu_{nf}}{\rho_{nf}} \quad (25)$$

$$\alpha_{nf} = \frac{k_{nf}}{(\square c_p)_{nf}} \quad (26)$$

In the above equations, φ is the volume fraction of nanoparticles, and the indices f and s represent fluid and nanoparticles, respectively. To calculate the effective thermal conductivity and viscosity, many models have been presented theoretically and experimentally. Maxwell and Brinkman separately presented equations for effective thermal conductivity and viscosity.

$$k_{nf} = k_f \times \frac{k_s + 2k_f + 2(k_s - k_f)\phi}{k_s + 2k_f - (k_s - k_f)\phi} \quad (27)$$

$$\mu_{nf} = \frac{\mu_f}{(1-\phi)^{2.5}} \quad (28)$$

As can be seen from the above equations, the properties of the nanofluid do not change with temperature. But in theory, the behavior of nanofluids is also represented by temperature-dependent equations and nanoparticle diameters. One of the equations that cover a wide range of nanofluid volume fraction and temperature is the equations presented, which is the Brownian motion for nanoparticles. The equations presented are as follows:

$$k_{nf} = k_{static} + k_{brownian} \quad (29)$$

$$k_{static} = k_f \times \frac{(k_s + 2k_f) - 2\varphi k_f - k_s}{(k_s + 2k_f) + \varphi(k_f - k_s)} \quad (30)$$

$$k_{brownian} = 5 \times 10^4 \beta\varphi\rho_f c_{pf} \sqrt{\frac{k_b T}{\rho_s d_s}} f(T, \varphi) \quad (31)$$

where β and f(T, φ) are presented as follows.

$$\beta = 0.0011\,(100\varphi)^{-0.7227} \quad \text{for } \varphi \geq 1\% \quad (32)$$

$$f(T, \varphi) = (-6.04\varphi + 0.4705)T + (1722.3\varphi - 134.63) \quad \text{for } 1\% \leq \varphi \leq 4\% \quad (33)$$

k_{static} is a static thermal conductivity based on Maxwell's classical equations, and $k_{Brownian}$ is to improve the heat conduction by heat convection of the buoyancy motion of nanoparticles. These equations are valid for temperatures between 300 K to 325 K.

Also, for effective viscosity, if the nanoparticles are spherical and rigid, the equations are given below.

$$\mu_{nf} = \mu_{static} + \mu_{brownian} \quad (34)$$

$$\mu_{static} = \frac{\mu_f}{(1-\varphi)^{2.5}} \quad (35)$$

$$\mu_{brownian} = 5 \times 10^4 \beta\varphi\rho_f \sqrt{\frac{k_b T}{\rho_s d_s}} f(T,\varphi) \quad (36)$$

4-Grid Study and Validation

This section presents the results of the grid independence study related to geometry. For this purpose, the average Nusselt numbers have been obtained for geometries with different sizes, and are compared in Table 4. For this purpose, geometries with different dimensions with the presence of all effective parameters should be used and the results should be checked. For this reason, φ= 2%, Ra = 105, the cavity slope is 30 degrees, and the bottom wall of the trapezoid is heated sinusoidally. According to the obtained values, it is observed that geometry with the number L×H=400×100 is suitable. The convergence criterion for the present study is considered as follows.

$$\frac{Nu_{avg}^{new} - Nu_{avg}^{old}}{Nu_{avg}^{old}} < 10^{-6} \quad (37)$$

Table 4: Grid study in this investigation for Ra = 10^5, φ =2% and $\Theta = 30°$

$Grid\ (L \times H)$	Nu_{avg}	CPU time (minutes)
40×160	2.8052	15
50×200	2.9532	19
80×320	3.0525	25
100×400	3.0958	40
120×480	3.0962	65

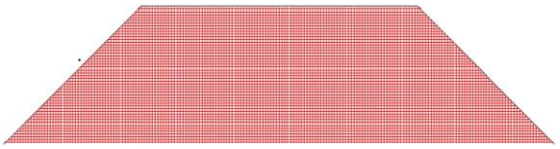

Fig. 4 Mesh generation

One of the requirements of numerical simulation is to confirm and validate the obtained results. This is achieved by solving a problem from previous valid research and matching it with the results obtained using a written numerical program. Using concepts such as nanofluid and magnetic field, valid references are used for this purpose. To validate the numerical program, the results of the numerical program written by Kefayati et al. [8], which simulate the mixed heat transfer of a flow nanofluid in the presence of a magnetic field inside a square cavity that is heated linearly, have been used. Nu_{avg} on the hot wall is compared between the present and reference work [8]. Good matching in this comparison in Table 5 indicates good performance of the written code.

Table 5: Comparison of the Nu_{avg} for present and reference results [8] in Ri = 100

Ha	Present Work	Kefayati et al. [8]
0	10.312	10.308
25	9.32	9.249
50	8.135	8.121
100	6.232	6.212

5- Natural Convection

According to the validation performed in the previous section, the results of the simulation of the problem presented in the problem statement are presented. The Rayleigh number, which is defined as follows, was explored in this work as a dimensionless number.

$$Ra = \frac{\rho \beta g L^3 \Delta T}{\alpha \mu} \quad (38)$$

which ρ is density, g is acceleration of cavity and μ is the viscosity of fluid. Table 7 shows the effect of volume fraction of nanoparticles and Ra number on the flow of natural heat transfer of fluid using the Nu_{avg} on the hot wall. In this simulation, no magnetic field is applied and a horizontal trapezoidal cavity is considered. The results show that in general, with increasing Ra number, the heat transfer inside the cavity increases. As can be seen from Table 7, by increasing the Ra number from $Ra = 10^3$ to $Ra = 10^5$, the Nu_{avg} at the bottom of the cavity increases significantly. And if in each Ra number, the volume fraction of nanoparticles changes from 0 to 3%, the Nu can increase by an average of 10%. Fig.7 shows that by adding Fe nanoparticles, the Nu_{avg} increases in all cases. But when the $Ra = 10^5$, by changing the volume fraction of nanoparticles from 2 to 3%, the Nu_{avg} decreases. As the percentage of the nanoparticles rises, this reduction may be brought about by a decrease in the Brownian motion of the particles. Then, as the nanoparticle size goes beyond 2%, the thermal conductivity starts to rise. An increase in diffusive heat transfer may be the source of this rise in thermal conductivity.

Table 7: Nu_{avg} of natural heat transfer of ethylene glycol-Fe nanofluids in *Ra*= 10^3 to 10^5 in φ =0 to 3% in the absence of magnetic field and zero cavity slope

φ	0%	1%	2%	3%
$Ra = 10^3$	1.8791	1.9391	2.0009	2.0630
$Ra = 10^4$	2.2636	2.3343	2.4002	2.4761
$Ra = 10^5$	3.5281	3.6212	3.7089	3.5062

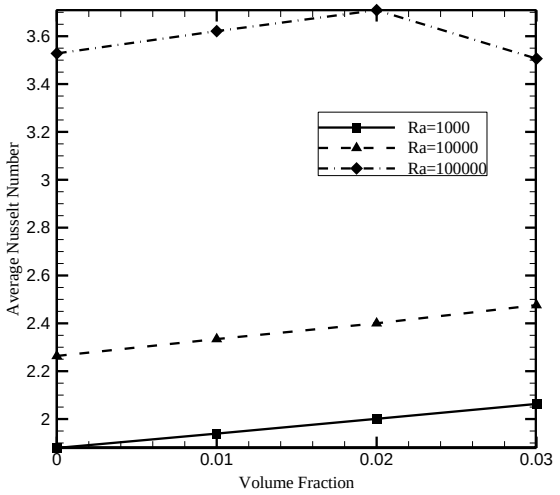

Fig. 7 Average Nusselt number diagram of natural heat transfer of ethylene glycol-Fe nanofluid in Ra= 10^3 to 10^5 in φ =0 to 3% in the absence of magnetic field and zero cavity slope

Fig. 8 shows the isothermal lines and streamlines in different Rayleigh numbers. It shows that with increasing Rayleigh number, the slope of the isothermal graph increases locally in the center of the trapezoidal cavity, which shows an increase in the rate of heat transfer in the middle of the cavity. This figure also shows that with increasing Ra number, the temperature in the center of the cavity increases, so that at $Ra = 10^3$ the temperature in the center of the cavity is equal to about 0.2 and at $Ra = 10^5$ the temperature is equal to about 0.3. As the Ra increases, the strength of the vortices inside the cavity increases dramatically. In all three Ra numbers are presented, there are two flow fronts in opposite directions and with relatively equal strength on both sides of the cavity, separated by a motionless space, which becomes smaller as the Ra number increases. By comparing streamlines and isothermal lines, it is clear that heat does not have much Thermal diffusivity in the parts surrounded by high-strength vortices, so in $Ra = 10^5$, two isothermal zones are located on the side walls. There are strong vortices in the contour of the streamlines.

Obviously, when there are high-strength vortices. flow does not moves to other parts so heat does not have thermal diffusivity.

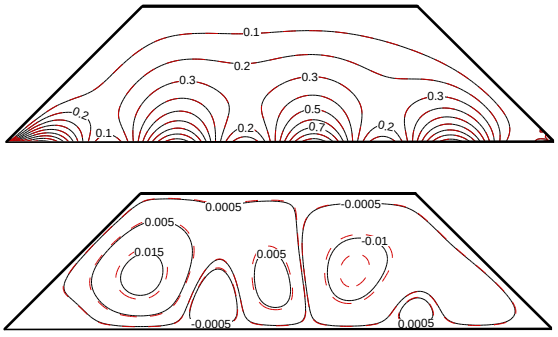

a: $Ra = 10^3$

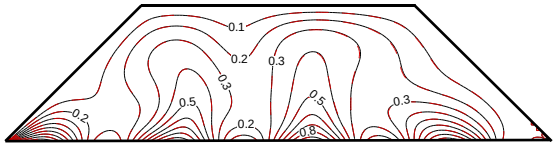

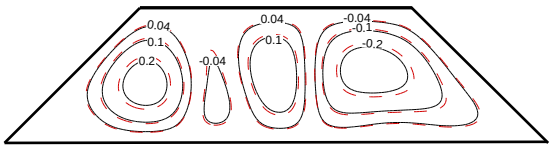

b: $Ra = 10^4$

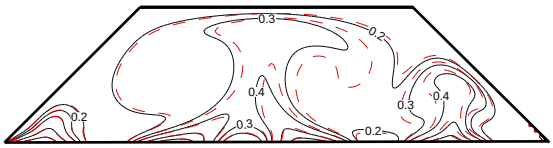

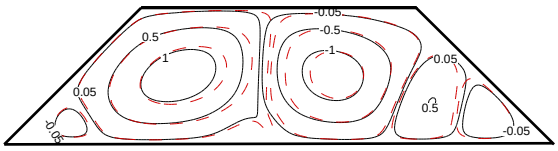

c: $Ra = 10^5$

Fig. 8 The isothermal and stream lines of natural heat transfer of ethylene glycol-Fe nanofluid in Ra= 10^3-10^5 and φ = 1,3% in the absence of magnetic field and chamber inclination of zero. (black solid lines for φ = 1% and reddashed lines for φ = 3%)

Table 7 shows the effect of cavity slope changes on streamlines and isothermal lines in $Ra = 10^3 - 10^5$ and φ =1%. This table states that at $Ra = 10^3$ little change occurs in the Nu_{avg}. While in higher Ra numbers the change of Nusselt number is more noticeable, as in $Ra = 10^4$ this change is equal to 7% and in $Ra = 10^5$ more than 20% difference is evident in different cases. By comparing isothermal lines, the different states are evident in Fig. 9, that when the $Ra = 10^3$, given that there is no high-power flow inside the cavity, there is little change in isothermal lines. But at higher Ra numbers, by changing the angle of the cavity, the vorticity power in the middle of the cavity is increased and does not allow thermal diffusivity to the top of the cavity. When $Ra = 10^3$ the effect of gravity is neglectable.

Table 8: The Nu_{avg} of heat transfer of ethylene glycol-Fe nanofluid in *Ra*=10^3 to 10^5 in φ =1, 3% in the absence of magnetic field and zero cavity slope

	Volume Fraction	Θ = 0°	Θ = 30°	Θ = 60°	Θ = 90°
$Ra = 10^3$	1%	2.0009	2.0026	2.002	1.9977
	3%	2.0630	2.012	2.021	2.0097
$Ra = 10^4$	1%	2.4002	2.4408	2.2645	2.2237
	3%	2.4761	2.4717	2.3317	2.2895
$Ra = 10^5$	1%	3.7089	3.0958	2.9698	2.8154
	3%	3.5062	3.0510	3.0510	2.8929

	Isotherms
Θ = 0°	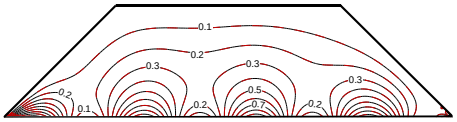
Θ = 30°	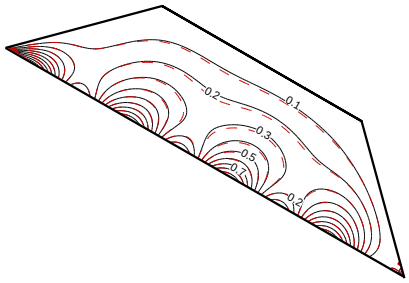
Θ = 60°	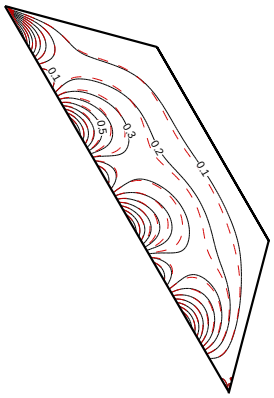
Θ = 90°	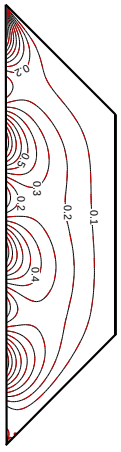

A: $Ra = 10^3$

	Isotherms
Θ = 0°	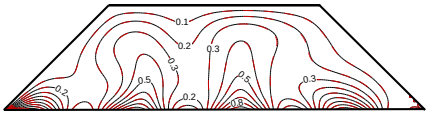
Θ = 30°	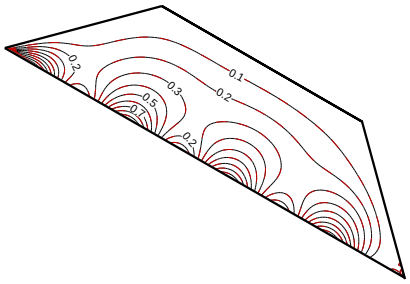
Θ = 60°	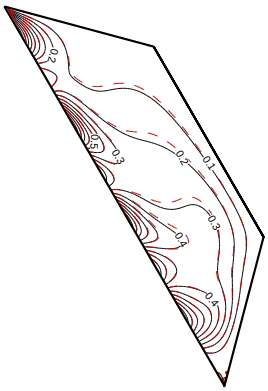
Θ = 90°	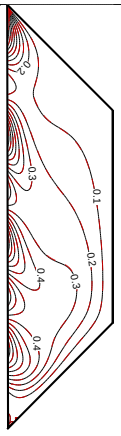

B: $Ra = 10^4$

	Isotherms
Θ = 0°	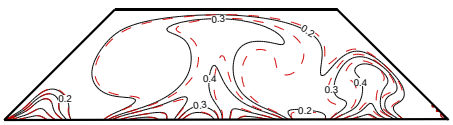

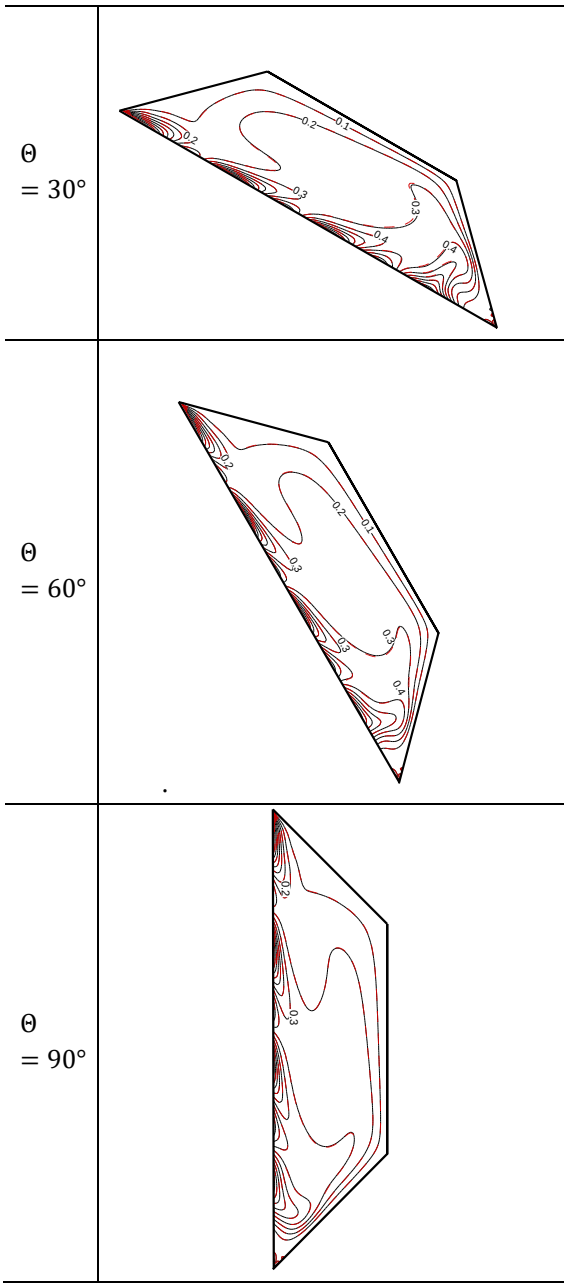

C: *Ra*= 10^5

Fig. 9 the isothermal of ethylene glycol-Fe nanofluid with φ =1,3% for different Ra numbers and θ= 0°-90° without magnetic field (black solid lines for φ = 1% and reddashed lines for φ = 3%)

Table 9 shows the effect of the Hartmann number on heat transfer in a trapezoidal cavity at φ = 2% in the presence of a magnetic field along the horizon. This table shows that with increasing Ha, the Lorentz force becomes stronger and in the opposite direction, the vertical component of velocity enters the nanofluid. Therefore, this force causes the effect of buoyancy force to be neutralized and therefore heat transfer is done at a lower rate in the cavity. Considering that at $Ra = 10^5$ the effect of buoyancy force is more effective than other Ra numbers. The application of a magnetic field has a greater effect on heat transfer, so that in $Ra = 10^3$ the effect of the application of a magnetic field with $Ha = 100$ is equal to 1% and in $Ra = 10^4$ and 10^5, this effect is equal to 17% and 44% respectively. Fig. 10 shows the reduction of the Nu_{avg} due to the application of different magnetic fields in different Ra numbers.

Table 9: Th Nu_{avg}e of natural heat transfer of ethylene glycol-Fe nanofluids in *Ra*= 10^3 to 10^5 at φ =0 to 3% and the zero cavity slope with the application of a magnetic field in Hartmann numbers between 0 and 100.

	Ha=0	Ha=50	Ha=100
$Ra = 10^3$	2.0009	1.9854	1.9844
$Ra = 10^4$	2.4052	2.0018	1.9907
$Ra = 10^5$	3.7089	2.3749	2.0759

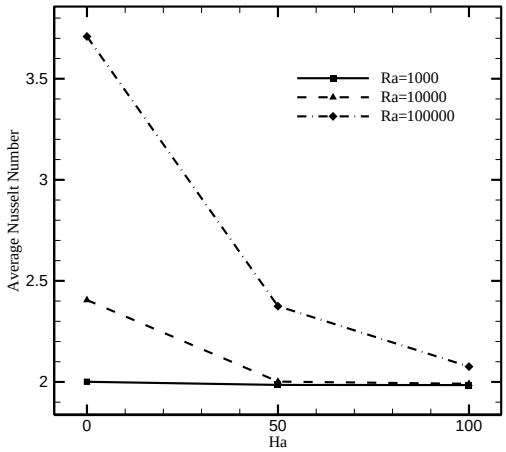

Fig. 10 Nu_{avg} diagram of natural heat transfer of ethylene glycol-Fe nanofluid in Ra= 10^3 to 10^5 in

$\varphi = 0$ to 3% and zero cavity slope by applying a magnetic field in Ha numbers between 0 to 100.

6- Conclusion

The effects of the magnetic field on natural and mixed heat transfer within a trapezoidal hollow that is sinusoidally heated from the bottom wall are investigated in this presentation. This research is numerically implemented using LBM, in which the magnetic field effect is incorporated to the force terms. In order to simulate the behavior of nanofluids, the temperature and nanoparticle diameter dependence equations are used. Also, in this research, the effect of changing various parameters such as Ri= 0.1-10, Ha= 0-100, φ =0-3%, slope of cavity (Θ) and angle of the magnetic field (γ) between (0°-90°) are studied. The findings suggest that raising the Rayleigh number while reducing the Richardson number increases heat transfer. Furthermore, raising the volume percentage of nanoparticles enhances the average Nusselt number by changing the other parameters. Furthermore, raising the Hartmann number decreases the velocity of flow within the cavity, reducing heat transfer. Changing the slope of the cavity and the angle of the applied magnetic field influences flow and heat transfer. The findings are summarized as follows:

- The improvement in Nu avg natural and mixed heat transfer results from the rise in nanoparticles' volume fraction.
- Increasing the Ra number also significantly improves heat transfer. When Ra is raised from Ra=103 to Ra=105, the Nuavg at the bottom of the cavity increases considerably. Additionally, the Nu can climb by 10% on average if the volume percentage of nanoparticles increases from 0% to 3% in each Ra number.
- As Ra increases, the temperature at the cavity's core increases as well, reaching a maximum of around 0.3 at Ra=105 and about 0.2 at Ra=103, respectively. Ra numbers cause the flow vortices inside the cavity to become more intense, which results in the creation of isothermal zones.
- As a result, the hot wall's temperature does not penetrate where strong vortices are present because of the movement of the cold wall.
- The stream and isothermal lines are affected by the inclined cavity's changing angle. The slope of the cavity has an impact on the streamlines as well. The effects of Ra are lessened by applying the magnetic field and increasing its strength. As a result, less heat is transferred. All natural and mixed heat transfers experience nearly the same amount of heat transfer in the presence of strong magnetic fields.

References

[1] Ashorynejad, H.R., Mohamad, A.A. and Sheikholeslami, M., 2013. Magnetic field effects on natural convection flow of a nanofluid in a horizontal cylindrical annulus using Lattice Boltzmann method. *International Journal of Thermal Sciences*, *64*, pp.240-250.

[2] Kahwaji, G., and Ali, O.M., "Numerical Investigation of Natural Convection Heat Transfer from Square Cylinder in an Enclosed Enclosure Filled with Nanofluids", International Journal of Recent Advances in Mechanical Engineering (IJMECH), Vol. 4, No. 4, pp. 1-17, (2015).

[3] Sheikholeslami, M., Gorji-Bandpy, M., and Ganji, D., "Lattice Boltzmann Method

for MHD Natural Convection Heat Transfer using Nanofluid", Powder Technology, Vol. 254, pp. 82-93, (2014).

[4] Choi, S.U.S., "Enhancing Thermal Conductivity of Fluids with Nanoparticles", ASME Fluids Engineering Division, Vol. 231, pp. 99-106, (1995).

[5] Heris, S.Z., Esfahany, M.N. and Etemad, S.G., 2007. Experimental investigation of convective heat transfer of Al2O3/water nanofluid in circular tube. *International journal of heat and fluid flow*, *28*(2), pp.203-210.

[6] Zarringhalam, M., Karimipour, A. and Toghraie, D., 2016. Experimental study of the effect of solid volume fraction and Reynolds number on heat transfer coefficient and pressure drop of CuO–water nanofluid. *Experimental Thermal and Fluid Science*, *76*, pp.342-351.

[7] Esfe, M.H., Saedodin, S., Mahian, O. and Wongwises, S., 2014. Efficiency of ferromagnetic nanoparticles suspended in ethylene glycol for applications in energy devices: effects of particle size, temperature, and concentration. *International Communications in Heat and Mass Transfer*, *58*, pp.138-146.

[8] Kefayati, G.R., Gorji-Bandpy, M., Sajjadi, H. and Ganji, D.D., 2012. Lattice Boltzmann simulation of MHD mixed convection in a lid-driven square cavity with linearly heated wall. *Scientia Iranica*, *19*(4), pp.1053-1065.

[9] Nemati, H., Farhadi, M., Sedighi, K., Fattahi, E. and Darzi, A.A.R., 2010. Lattice Boltzmann simulation of nanofluid in lid-driven cavity. *International Communications in Heat and Mass Transfer*, *37*(10), pp.1528-1534.

[10] Hasib, M.H., Hossen, M.S. and Saha, S., 2015. Effect of tilt angle on pure mixed convection flow in trapezoidal cavities filled with water-Al2O3 nanofluid. *Procedia Engineering*, *105*(1), pp.388-397.

[11] Ma, Y., Mohebbi, R., Rashidi, M.M., Yang, Z. and Sheremet, M., 2020. Nanoliquid thermal convection in I-shaped multiple-pipe heat exchanger under magnetic field influence. *Physica A: Statistical Mechanics and its Applications*, *550*, p.124028.

[12] Sheikholeslami, M., Gorji-Bandpy, M., and Ganji, D., "Lattice Boltzmann Method for MHD Natural Convection Heat Transfer using Nanofluid", Powder Technology, Vol. 254, pp. 82-93, (2014).

[13] Mliki, B., Abbassi, M.A., Guedri, K., and Omri, A., "Lattice Boltzmann Simulation of Natural Convection in an L-Shaped Enclosure in the Presence of Nanofluid", Engineering Science and Technology, an International Journal, Vol. 18, pp. 503-511, (2015).

[14] Jafari, M., Farhadi, M., Akbarzade, S., and Ebrahimi, M., "Lattice Boltzmann Simulation of Natural Convection Heat Transfer of SWCNT-Nanofluid in an Open Enclosure", Ain Shams Engineering Journal, Vol. 6, pp. 913-927, (2015).

[15] Chamkha, A.J., and Ismael, M.A., "Magnetic Field Effect on Mixed Convection in Liddriven Trapezoidal Cavities Filled with a Cu–water Nanofluid with an Aiding or Opposing Side Wall", Journal of Thermal Science and Engineering Applications, Vol. 8, pp. 310-319, (2016).

[16] Mahmoudi, A., Mejri, I., Abbassi, M.A., and Omri, A., "Lattice Boltzmann Simulation of MHD Natural Convection in a Nanofluid-filled Cavity with Linear Temperature Distribution", Powder Technology, Vol. 256, pp. 257-271, (2014).

[17] Kefayati, G.R., Gorji-Bandpy, M., Sajjadi, H. and Ganji, D.D., 2012. Lattice Boltzmann simulation of MHD mixed convection in a lid-driven square cavity with linearly heated wall. *Scientia Iranica*, *19*(4), pp.1053-1065.

[18] Ma, Y., Rashidi, M.M., Mohebbi, R. and Yang, Z., 2020. Nanofluid natural convection in a corrugated solar power plant using the hybrid LBM-TVD method. *Energy*, *199*, p.117402.

[19] Mehryan, S.A.M., Izadpanahi, E., Ghalambaz, M. and Chamkha, A.J., 2019. Mixed convection flow caused by an oscillating cylinder in a square cavity filled with Cu–Al2O3/water hybrid nanofluid. *Journal of Thermal Analysis and Calorimetry*, 137(3), pp.965-982.

[20] Bellout, S. and Bessaïh, R., 2021. Heat Transfer Improvement in an Open Cubic Cavity using a Hybrid Nanofluid. *Journal of Applied and Computational Mechanics*, 7(3), pp.1501-1513.

[21] Mehryan, S.A.M., Ghalambaz, M., Chamkha, A.J. and Izadi, M., 2020. Numerical study on natural convection of Ag–MgO hybrid/water nanofluid inside a porous enclosure: A local thermal non-equilibrium model. *Powder Technology*, 367, pp.443-455.

[22] Mehryan, S.A.M., Ghalambaz, M., Gargari, L.S., Hajjar, A. and Sheremet, M., 2020. Natural convection flow of a suspension containing nano-encapsulated phase change particles in an eccentric annulus. Journal of Energy Storage, 28, p.101236.

[23] Rahman, A., Redwan, D.A., Thohura, S., Kamrujjaman, M. and Molla, M.M., Natural convection and entropy generation of non-Newtonian nanofluids with different angles of external magnetic field using GPU accelerated MRT-LBM. *Case Studies in Thermal Engineering*, p.101769, 2022.

[24] Rahimi, A., Kasaeipoor, A., Malekshah, E.H. and Amiri, A., 2018. Natural convection analysis employing entropy generation and heatline visualization in a hollow L-shaped cavity filled with nanofluid using lattice Boltzmann method-experimental thermo-physical properties. Physica E: Low-Dimensional Systems and Nanostructures, 97, pp.82-97.

[25] Hussein, A.K., Lioua, K., Chand, R., Sivasankaran, S., Nikbakhti, R., Li, D., Naceur, B.M. and Habib, B.A., 2016. Three-dimensional unsteady natural convection and entropy generation in an inclined cubical trapezoidal cavity with an isothermal bottom wall. *Alexandria Engineering Journal*, *55*(2), pp.741-755.

[26] Armaghani, T., Esmaeili, H., Mohammadpoor, Y.A. and Pop, I., 2018. MHD mixed convection flow and heat transfer in an open C-shaped enclosure using water-copper oxide nanofluid. *Heat and Mass Transfer*, *54*(6), pp.1791-1801.

[27] Zhang, X., Xu, Y., Zhang, J., Rahmani, A., Sajadi, S.M., Zarringhalam, M. and Toghraie, D., 2021. Numerical study of mixed convection of nanofluid inside an inlet/outlet inclined cavity under the effect of Brownian motion using Lattice Boltzmann Method (LBM). *International Communications in Heat and Mass Transfer*, *126*, p.105428.